

Incorporation-related structural issues for beryllium doping during growth of GaN by rf-plasma molecular-beam epitaxy

A. J. Ptak, Lijun Wang, N. C. Giles, and T. H. Myers^{a)}

Physics Department, West Virginia University, Morgantown, West Virginia 26506

L. T. Romano^{b)}

Xerox Palo Alto Research Center, Palo Alto, California 94304

C. Tian, R. A. Hockett, S. Mitha, and P. Van Lierde

Evans Analytical Group, Charles Evans and Associates, Sunnyvale, California 94086

(Received 4 June 2001; accepted for publication 18 October 2001)

Beryllium incorporation was studied for both Ga-polarity and N-polarity GaN using a series of Be step-doped epitaxial layers. Dopant concentration profiles indicated that surface polarity-related incorporation differences are not pronounced for Be. Significant surface accumulation of Be occurs during growth with surface accumulations approaching a monolayer for heavier doping levels. Transmission electron microscopy studies indicate the surface layer of Be has a significant effect on the microstructure, particularly for near monolayer coverage. © 2001 American Institute of Physics. [DOI: 10.1063/1.1429290]

While magnesium is currently the most technologically important *p*-type dopant for GaN, Be also shows promise. Although there have been several studies concerning Be as a dopant in GaN,^{1–4} little information has emerged concerning either Be incorporation mechanisms during growth by molecular-beam epitaxy (MBE) or the effect of Be on structural properties. We present the results of a study of Be incorporation for both N- and Ga-polarity GaN that strongly indicates surface accumulation occurs, and that strain introduced by the surface layer affects structural properties which may limit Be doping.

The Be-doped GaN layers were grown at West Virginia University (WVU) by rf plasma-assisted MBE using techniques reported previously.⁵ N-polarity GaN was obtained by nucleating GaN buffer layers directly on sapphire under heavily Ga-rich conditions.⁶ Incorporation in Ga-polarity GaN was studied by growth on metalorganic chemical vapor deposition (MOCVD) GaN templates on (0001) sapphire substrates. Step-doped structures were produced through opening and closing the dopant shutter. All changes in oven and substrate temperatures occurred with the dopant shutter closed. Secondary ion mass spectrometry (SIMS) measurements were performed by Evans Analytical Group. Room temperature Raman spectroscopy was performed at WVU using a Jobin–Yvon Ramanor U-1000 micro-Raman system excited by 476-nm laser light. Cross section transmission electron microscopy (XTEM) studies were performed at Xerox using a JEOL 3010 microscope following previously published procedures.⁷

Figure 1 shows a SIMS profile of Be obtained from a Ga-polarity step-doped sample. The general features observed in this profile are representative of all the structures investigated. By monitoring the growth rate throughout layer

growth with laser interferometry and using other chemical markers measured in SIMS, the correlation with the shutter is accurate within an uncertainty of 100 nm. The Be incorporation increases with increasing oven temperature consistent with changes in the Be vapor pressure. By comparing expected profiles to the measured Be incorporation, the Be appears to segregate and accumulate on the surface. There is a continual increase in Be incorporation while the shutter is open with the highest Be concentration occurring at the point the shutter is closed. Such profiles, indicative of surface accumulation, were observed for all growth conditions. Indeed, for Ga-polarity step-doped structures at concentrations less than 10^{17} cm⁻³, there is actually a pronounced lack of any step-like structure relating to the opening and closing of the Be shutter similar to what has been reported for Mg and consistent with a mechanism for stable surface accumulation.⁵ Auger electron spectroscopy measurements performed on several step-doped and uniformly doped layers also indicated the presence of Be at the surface. Although

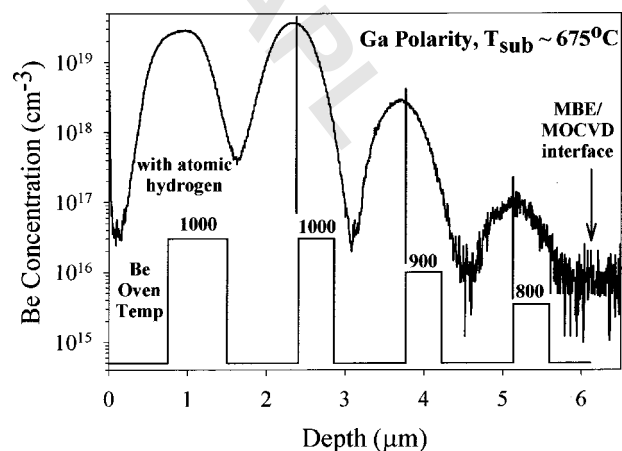


FIG. 1. SIMS measurement showing the Be incorporated into a Ga-polar sample. Shown schematically are the opening and closing positions of the Be shutter, as well as the Be furnace temperatures.

^{a)}Electronic mail: tmyers@wvu.edu

^{b)}Current address: Novacrystals, San Jose, California 95131; Electronic mail: linda_romano@novacrystals.com

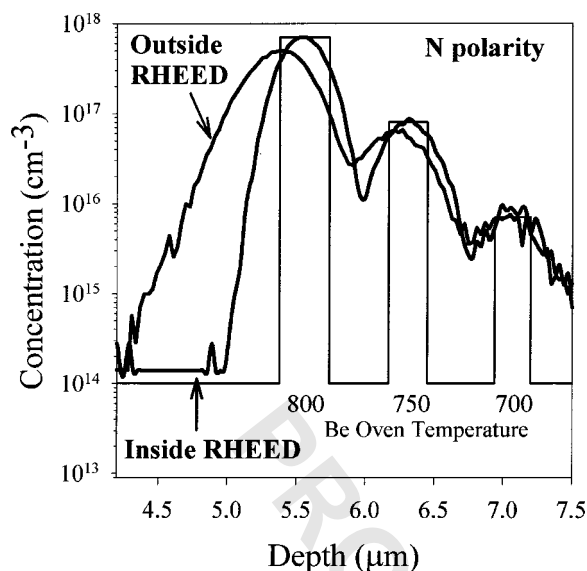


FIG. 2. SIMS measurement of Be inside and just outside the stripe created by the electron irradiation of the RHEED beam. The high-energy electrons appear to suppress surface accumulation.

quantitative interpretation was complicated, the presence of Be was measured to be at levels representing a significant fraction of a monolayer.

The last doping step shown in Fig. 1 was grown under atomic hydrogen from a thermal cracker. When the increase in growth rate due to atomic H is taken into account,⁸ there does not appear to be a significant difference in Be incorporation. That is, the same number of Be atoms were incorporated with and without hydrogen for identical time intervals. Unlike the case for Mg,⁹ hydrogen is incorporated at levels at or above the Be concentration for growth under atomic H. This finding suggests that the Be–H bond may be stronger than the Mg–H bond, as predicted by recent calculations,¹⁰ since Mg doping can be accomplished under a similar atomic hydrogen flux without significant H incorporation.⁹ Thus, removal of H through thermal annealing in Be-doped GaN may be more problematic than with Mg doping. Other mechanisms leading to enhanced H incorporation are possible, however.

Further SIMS measurements on N-polarity films grown directly on sapphire (not shown) indicate that Be incorporation is similar to Ga-polarity films for a similar flux, in contrast to the significant polarity incorporation difference observed for Mg doping.⁹ Also unlike Mg, Be incorporation is not a strong function of substrate temperature at higher concentrations with the same incorporation levels occurring for temperatures between 550 °C and 700 °C. Some temperature dependence is present at low concentrations. Again unlike the case for Mg, incorporation rates do not change significantly when going from very Ga-stable growth conditions to N-stable growth.

On many N-polarity samples, evidence of a stripe occurring during reflection high-energy electron diffraction (RHEED) is one of the previously reported effects that electron irradiation can have during MBE growth.¹¹ Of interest, Fig. 2 contains a comparison between the measured Be concentration profiles inside and just outside such a RHEED stripe. The total number of Be atoms incorporated for each

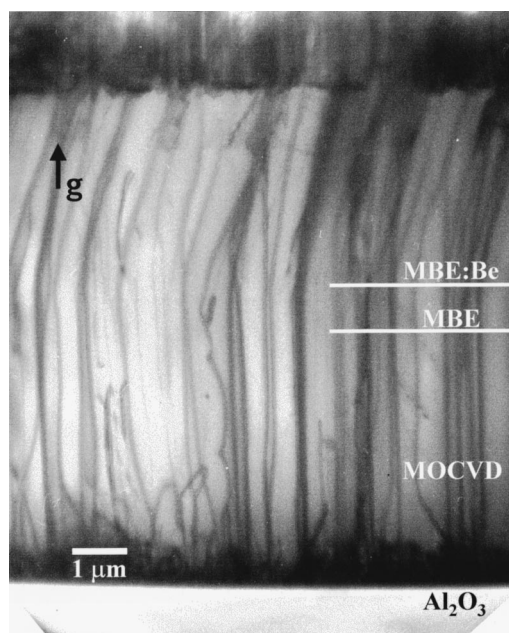


FIG. 3. TEM bright field micrograph of a Be step-doped film grown by MBE on a MOCVD template taken with diffraction vector $g=0002$ near the $[11\bar{2}0]$ zone axis.

step is the same in each case and yet the Be profiles for the electron irradiated portion closely matches the shutter profile and exhibits a classical diffusion profile. Thus, it appears electron irradiation suppresses surface accumulation of Be allowing an estimate of an upper limit for the Be diffusion coefficient for this temperature (675 °C) of $1 \times 10^{-15} \text{ cm}^2 \text{ s}^{-1}$ following standard analysis of diffusion of a step-doped profile and the time at temperature during growth.¹² An estimate of the number of Be atoms on the sample surface can be obtained with some confidence by counting the Be incorporated after the doping shutter is closed and accounting for the effect of diffusion on the profile. Analysis of the profiles shown in Fig. 1 indicates 3×10^{12} , 7×10^{13} and 8×10^{14} Be atoms/cm² accumulated on the GaN surface for Be oven temperatures of 800 °C, 900 °C, and 1000 °C, respectively, at the time the shutter is closed. For equivalent doping of N-polarity GaN, surface concentrations of 2×10^{12} , 5×10^{13} and 7×10^{14} Be atoms/cm² were observed. These numbers indicate a high surface concentration of Be, consistent with both the SIMS and the Auger results. Indeed, the largest surface accumulation corresponds to essentially a monolayer of Be residing on the surface.

XTEM was performed on several of the step-doped layers. Figure 3 is a TEM micrograph of the step-doped sample with the SIMS profile shown in Fig. 1. The MBE layer was grown on an MOCVD template with no structural evidence of an interface between the MOCVD and MBE material. Threading dislocations originating in the MOCVD layer, typically stable for growth along the c -axis, proceed without interruption into the MBE layer. However, when Be is first introduced into the growing MBE layer at a level of about 10^{17} cm^{-3} , the dislocations are unexpectedly seen to bend at an angle of $\sim 70^\circ$ from the basal plane. This angle is not consistent with a low index plane in the hexagonal lattice and therefore may result from the morphology developed during growth related to Be surface accumulation. The

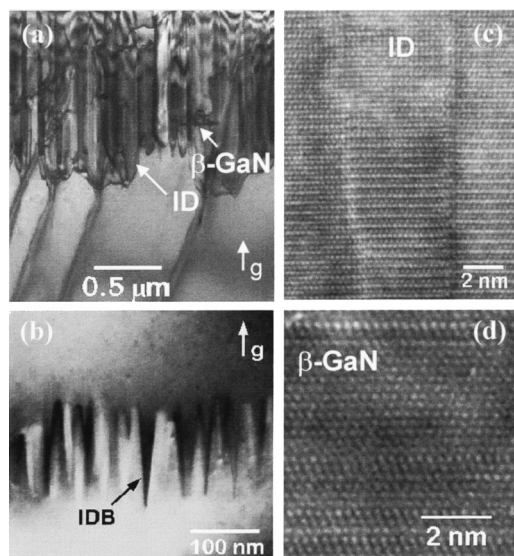


FIG. 4. TEM micrographs of the upper defect layer shown in Figs. 3 (a) and 3(c) are bright and dark field micrographs, respectively, taken with $g=0002$, revealing ID, cubic β -GaN, and IDBs. (b) and (d) are high resolution images of an ID and a region of β -GaN.

“bent” dislocations propagate at this angle without an observable change either due to the closing of the Be shutter, thereby decreasing the Be concentration, or the subsequent opening of the shutter which results in Be incorporation at levels up to 10^{18} cm^{-3} . When Be was incorporated at levels of $\sim 5 \times 10^{19} \text{ cm}^{-3}$, a very high density of planar defects was observed as clearly seen in Fig. 3 as the dark region near the sample surface.

Figure 4 illustrates this planar defect structure consisting mainly of inversion domains (ID) for Ga-polarity samples, similar to observations for heavy Mg doping in both MOCVD and MBE.¹³ The inversion does not take place uniformly along the surface but forms isolated inversion domain boundaries (IDB) along the $\{1010\}$ planes as shown in Figs. 4(a) and 4(b). The IDB forms a steep facet $\sim 10^\circ$ from the basal plane normal at the bottom. Figure 4(c) is a (0002) dark field TEM image of an IDB that extends over several hundreds of nanometers. Defects observed parallel to the basal plane were regions of cubic GaN, as shown in Fig. 4(d). The cubic slabs were typically less than 10 nm thick and up to $\sim 0.5 \mu\text{m}$ in length. Although not present in Fig. 3, a significant number of microcracks were also observed in the heavily doped region. Structural degradation also occurs for N-polar samples at the high Be concentration with the exception that polarity inversion is not observed (not shown). In the N-polar case, the threading dislocation density increased and a significant density of microcracks was again observed in the heavily doped regions, suggesting that strain plays a role in the degradation. SIMS measurements indicate that oxygen and carbon are at levels less than the background levels (low-to-mid 10^{16} cm^{-3}) in both polarities of the Be-doped samples. Thus, O and C are not contributing to this defect formation.

Raman spectroscopy measurements^{14,15} were made on uniformly Be-doped layers consisting of a $1 \mu\text{m}$ thick Be-doped layer grown on a $2 \mu\text{m}$ thick MOCVD layer. The measured shift in the E_2 Raman peak (at $\sim 570 \text{ cm}^{-1}$) was thus indicative of strain in the composite system. Measure-

ments for Be concentrations up to 10^{18} cm^{-3} indicated negligible strain difference when compared to undoped layers. In contrast, measurements on samples with Be concentrations near the onset of degradation ($\sim 4 \times 10^{19} \text{ cm}^{-3}$) indicated a significant increase in compressive strain (up to 0.001) for the composite system.

The strain measured by Raman and the observation of microcracks by TEM indicates that the large measured Be surface concentration may be responsible for the large compressive strain. This strain could affect the surface morphology resulting in the bent dislocations in Fig. 3. At the highest doping levels, with surface coverage of Be approaching a complete monolayer, both IDs and regions of cubic GaN form on the Ga polarity, while significant dislocation multiplication and microcracks occur on the N polarity. These effects may occur in an attempt to relieve surface strain. Of course, the large Be coverage itself may cause the IDs to form, similar to Mg doping,¹⁶ and lead to the formation of the cubic phase. Regardless of the mechanism, surface accumulation of Be under standard GaN growth conditions by MBE ultimately leads to a breakdown of structural quality, and sets a limit on the maximum Be concentration attainable. It is of interest that the phenomenon of structural degradation was observed for Be doping of cubic GaN³ at similar incorporation levels, $\sim 10^{20} \text{ cm}^{-3}$.

In summary, Be incorporation is well behaved with the egregious exception that significant surface accumulation occurs during most standard MBE growth conditions. Strain associated with this surface layer affects structural properties as measured by TEM. Surface layers approaching a monolayer coverage result in severe structural degradation during growth, limiting maximum Be concentrations to less than the mid- 10^{19} cm^{-3} level. Nonstandard growth approaches may be necessary for Be doping in GaN. The apparent suppression of Be surface accumulation by electron irradiation is certainly intriguing.

This work was supported at WVU by ONR Grant No. N00014-96-1-1008 and at WVU and Xerox-PARC by ONR Contract No. N00014-99-C-0161.

¹M. A. Sanchez-Garcia, E. Calleja, F. J. Sanchez, F. Calle, E. Monroy, D. Basak, E. Munoz, C. Villar, A. Sanz-Hervas, M. Aguilar, J. J. Serrano, and J. M. Blanco, *J. Electron. Mater.* **27**, 276 (1998).

²D. J. Dewsnip, A. V. Andrianov, I. Harrison, J. W. Orton, D. E. Lacklison, G. B. Ren, S. E. Hooper, T. S. Cheng, and C. T. Foxon, *Semicond. Sci. Technol.* **13**, 500 (1998).

³K. H. Ploog and O. Brandt, *J. Vac. Sci. Technol. A* **16**, 1609 (1998).

⁴A. Salvador, W. Kim, O. Atkas, A. Botchkarev, Z. Fan, and H. Morkoc, *Appl. Phys. Lett.* **69**, 2692 (1996).

⁵T. H. Myers, A. J. Ptak, Lijun Wang, and N. C. Giles, *Inst. Pure Appl. Phys. Conf. Series* **1**, 451 (2000).

⁶Z. Yu, S. L. Buczkowski, N. C. Giles, T. H. Myers, and M. R. Richards-Babb, *Appl. Phys. Lett.* **69**, 2731 (1996).

⁷L. T. Romano, J. E. Northrup, and M. A. O’Keefe, *Appl. Phys. Lett.* **69**, 2394 (1996).

⁸A. J. Ptak, M. R. Millecchia, T. H. Myers, K. S. Ziemer, and C. D. Stinespring, *Appl. Phys. Lett.* **74**, 3836 (1999).

⁹A. J. Ptak, T. H. Myers, L. T. Romano, C. G. Van de Walle, and J. E. Northrup, *Appl. Phys. Lett.* **78**, 285 (2001).

¹⁰C. G. Van de Walle, S. Limpijumnong, and J. Neugebauer, *Phys. Rev. B* **63**, 245205 (2001).

¹¹B. L. VanMil, A. J. Ptak, N. C. Giles, T. H. Myers, P. J. Treado, M. P. Nelson, J. M. Ribar, and R. D. Smith, *J. Vac. Sci. Technol. B* **18**, 2295 (2000).

- ¹²*The Mathematics of Diffusion* by J. Crank (Clarendon, Oxford, 1975), p. 15.
- ¹³V. Ramachandran, R. M. Feenstra, W. L. Sarney, L. Salamanca-Riba, J. E. Northrup, L. T. Romano, and D. W. Greve, *Appl. Phys. Lett.* **75**, 808 (1999).
- ¹⁴V. Yu. Davydov, N. S. Averkiev, I. N. Goncharuk, D. K. Nelson, I. P. Nikitina, A. S. Polkovnikov, A. N. Smirnov, and M. A. Jacobson, *J. Appl. Phys.* **82**, 5097 (1997).
- ¹⁵L. T. Romano, C. G. Van de Walle, J. W. Ager III, W. Gotz, and R. S. Kern, *J. Appl. Phys.* **87**, 7745 (2000).
- ¹⁶L. T. Romano, J. E. Northrup, A. J. Ptak, and T. H. Myers, *Appl. Phys. Lett.* **77**, 2479 (2000).

PROOF COPY 047152APL